Metallophysics and Advanced Technologies
Металофіз. новітні технол.
Metallofiz. Noveishie Tekhnol.
2026, vol. 48, No. 9, pp. 973–983
https://doi.org/10.15407/mfint.48.09.0973
Reprints available directly from the publisher

© 2026 G. V. Kurdyumov Institute for Metal Physics,
National Academy of Sciences of Ukraine
Published by license under
the G. V. Kurdyumov Institute for Metal Physics–
N.A.S. of Ukraine Publishers imprint.
Printed in Ukraine.

PACS numbers: 61.66.Dk, 68.37.Hk, 81.05.Bx, 81.20.Ev, 81.30.Hd, 81.40.Cd, 81.70.Pg

Mechanism of *in situ* WC Formation during Mechanical Alloying of the Medium-Entropy $W_{1.5}$FeCoNi Alloy

S. Yu. Teslia[*], O. I. Yurkova[*], D. S. Leonov[**], and P. I. Loboda[*]

[*]*National Technical University of Ukraine*
'Igor Sikorsky Kyiv Polytechnic Institute',
37, Beresteiskyi Ave., UA-03056 Kyiv, Ukraine
[**]*Technical Center, N.A.S. of Ukraine,*
13, Pokrovs'ka Str., UA-04070 Kyiv, Ukraine [1]

Mechanical alloying in a high-carbon medium (petroleum) is used to fabricate a $W_{1.5}$FeCoNi medium-entropy alloy (MEA) *in situ* reinforced by tungsten carbide (WC). During high-energy ball milling of a mixture of elemental metal powders (W, Fe, Co and Ni) for 20 hours, a b.c.c. solid solution and dispersed WC particles with a grain size from 0.5 μm to 1 μm are formed. The carbide-phase formation involves the decomposition of petrol, the generation of carbon radicals, and a subsequent reaction with tungsten that leads to the formation of WC by both direct reaction with W particles and diffusion into the b.c.c. lattice. XRD and SEM analyses reveal gradual alloying, crystallite refinement, and homogenization of a b.c.c. solid-solution matrix. DSC measurements show two endothermic peaks at 885°C and 1040°C, corresponding to short-range ordering, sintering of the powder, secondary WC precipitation, and randomization of a solid solution with possible b.c.c.–f.c.c. transformations. The *in situ* carbide reinforcement and uniform microstructure are expected to enhance significantly the mechanical properties and thermal stability of the MEA, demonstrating the feasibility of this approach for high-performance carbide-strengthened alloys.

Key words: high-entropy materials, mechanical alloying, tungsten carbide.

Corresponding authors: Serhii Yuriyovych Teslia
E-mail: teslia.serhii@lll.kpi.ua

Citation: S. Yu. Teslia, O. I. Yurkova, D. S. Leonov, and P. I. Loboda, Mechanism of *in situ* WC Formation during Mechanical Alloying of the Medium-Entropy $W_{1.5}$FeCoNi Alloy, *Metallofiz. Noveishie Tekhnol.*, 48, No. 9: 973–983 (2026), DOI: 10.15407/mfint.48.09.0973

© Publisher PH 'Akademperiodyka' of the NAS of Ukraine, 2026. This is an open access article under the CC BY-ND license (https://creativecommons.org/licenses/by-nd/4.0)

Методу механічного леґування у висококарбоновому середовищі (бензині) було використано для одержання стопу середньої ентропії (MEA) складу $W_{1.5}FeCoNi$, зміцненого карбідом Вольфраму (WC) безпосередньо в процесі синтези (*in situ*). Під час високоенергетичного кульового помелу суміші елементних металевих порошків (W, Fe, Co і Ni) упродовж 20 годин утворилися твердий розчин із ОЦК-структурою та дисперсні частинки WC із розміром зерен від 0,5 до 1 мкм. Процес утворення карбідної фази включає розкладання бензину, ґенерацію вуглецевих радикалів і подальшу реакцію з вольфрамом, що приводить до формування WC, як шляхом безпосередньої взаємодії з частинками W, так і внаслідок дифузії в ОЦК-ґратницю. Методи рентґенофазової аналізи (XRD) та сканувальної електронної мікроскопії (SEM) виявили поступове леґування, подрібнення кристалітів і гомогенізацію матриці твердого розчину з ОЦК-структурою. Результати диференційної сканувальної калориметрії (DSC) показали наявність двох ендотермічних піків при 885°C і 1040°C, що відповідають процесам близького впорядкування, спікання порошку, вторинного виділення WC і розупорядкування твердого розчину з можливими фазовими перетвореннями типу ОЦК–ГЦК. Очікується, що зміцнення карбідами (*in situ*) та формування однорідної мікроструктури значно поліпшать механічні властивості та термічну стабільність цього стопу, що підтверджує доцільність застосування такого підходу для створення високоефективних стопів, зміцнених карбідами.

Ключові слова: високоентропійні матеріяли, механічне леґування, карбід Вольфраму.

(Received 14 September, 2026; in final version, 18 September, 2026)

1. INTRODUCTION

High-entropy alloys (HEAs) represent a novel class of metallic materials that exhibit an exceptional balance of high hardness and strength, along with sufficient ductility and outstanding resistance to wear, corrosion, and oxidation [1–3]. Due to their high configurational entropy, HEAs typically form single, two-phase, or multiphase solid solutions rather than intermetallic compounds. This distinctive characteristic opens new opportunities for the application of these alloys in many fields, particularly in environments with high temperatures [4, 5]. The extraordinary properties of HEAs are provided for their application as a binder in metal–ceramic composites strengthened with refractory compounds [6–9]. The concept of strengthening high-entropy alloys through the formation of composite structures can be realized either *ex situ*, by adding ceramic reinforcements (oxides, borides, carbides) [7, 8, 10], or *in situ*, during thermal ageing [11] or through chemical reactions with non-metallic doping such as B [12, 13], [14], C [15, 16], N [17, 18], and O [19, 20]. Bharat Gwalani *et al.* [21] found that *ex situ* adding of 3 vol.% Y_2O_3 to $Al_{0.3}CoCrFeMnNi$ resulted in a

significant increase in compressive yield strength from 979 MPa to 1759 MPa. In the study [22], the effect of the amount of SiC) on phase composition and mechanical properties of f.c.c. CoCrFeNi was shown. Incorporation of SiC particles led not only to a substantial increase in the yield strength but also to the preservation of considerable ductility. The HEA composite with 6 wt.% SiC reached yield strength of ≅ 1200 MPa, over eight times which of the base alloy (200 MPa), while maintaining an elongation of 37%. Compared to *ex situ* methods, the *in situ* formation of reinforcing phases is preferable because it ensures a cleaner interface and stronger bonding between the matrix and the formed phase, leading to improved mechanical and thermal properties. It is well known that the appropriate addition of interstitial elements with small atomic radii in traditional alloys, such as steels and superalloys, is beneficial to their structure and properties. The interstitial atoms cause evident lattice distortion in HEAs, which affects significantly the interaction between dislocations and other crystal defects and in addition, if the solubility of non-metal atoms in the HEA matrix is exceeded, carbides, nitrides, borides can form, which will lead to greater microstructure refinement (and dispersion strengthening of alloys [23–26]. Among known refractory compounds, tungsten carbide is one of the most promising strengthening phases, because it combines high hardness and thermal stability with good chemical resistance, providing effective strengthened of the matrix even at high temperatures and in aggressive environments [27].

In this study, we proposed a new method to fabricate *in situ* carbide-strengthened $W_{1.5}$FeCoNi medium-entropy alloy (MEA) by mechanical alloying in a high-carbon medium (petrol). The use of iron-group metals for MEA preparation is due to the low solubility of carbon, low price, and solid-solution stabilization.

2. MATERIALS AND METHODS

The initial powders were commercially available, which was W (2–6 μm, > 99.95% purity, Vimaterial), Fe (ASC100.29, 20–45 μm, > 99.91% purity, Höganäs), Co (2–4 μm, > 99.8% purity, ChemPur), Ni (2–4 μm, > 99.7% purity ChemPur). A portion of powder was placed in the cemented carbide jar and mechanically alloyed (MA) at a speed of 400 rpm/min for duration of 20 h. To prevent the oxidation of powders during high-energy milling, high-purity argon was introduced into the ball mill jar. The ball-to-powder mass ratio was 10:1. Petrol was used as a carbon source to form *in situ* WC-carbide particles and as a processing controlling agent to avoid excessive cold welding. The evolution of phase composition and powder microstructure was investigated after 1, 2, 10, 15 and 20 h of MA. The structure and phase transformations were investigated by x-ray diffractometer Ultima IV (Rigaku

Corp., Tokyo, Japan) at 30 kV and 15/20 mA in the range $2\theta = 20–90°$. Structural parameters were refined by the Rietveld method using the PDXL software. A scanning electron microscope (SEM) Axia ChemiSEM LoVac was used to obtain basic information concerning microstructure of the powder particles. The chemical composition of the alloy was determined, using energy dispersive x-ray (EDX) microanalysis in a SEM equipped with an energy-dispersive detector TrueSight X. Differential scanning calorimeter (DSC, DSC PT 1600 — Linseis, Germany) was used to analyse the thermal stability of $W_{1.5}FeCoNi$ alloy under flowing argon atmosphere. The scanning ranges were 25–1250°C at a heating rate of 10°C/min in the Al_2O_3 crucible.

3. RESULTS AND DISCUSSION

The XRD results (Fig. 1, *a*) indicate that the b.c.c. solid solution and WC phase and were formed after 20 h of MA. At the initial stage of MA, after 1–2 h, a clear broadening and a significant decrease in the

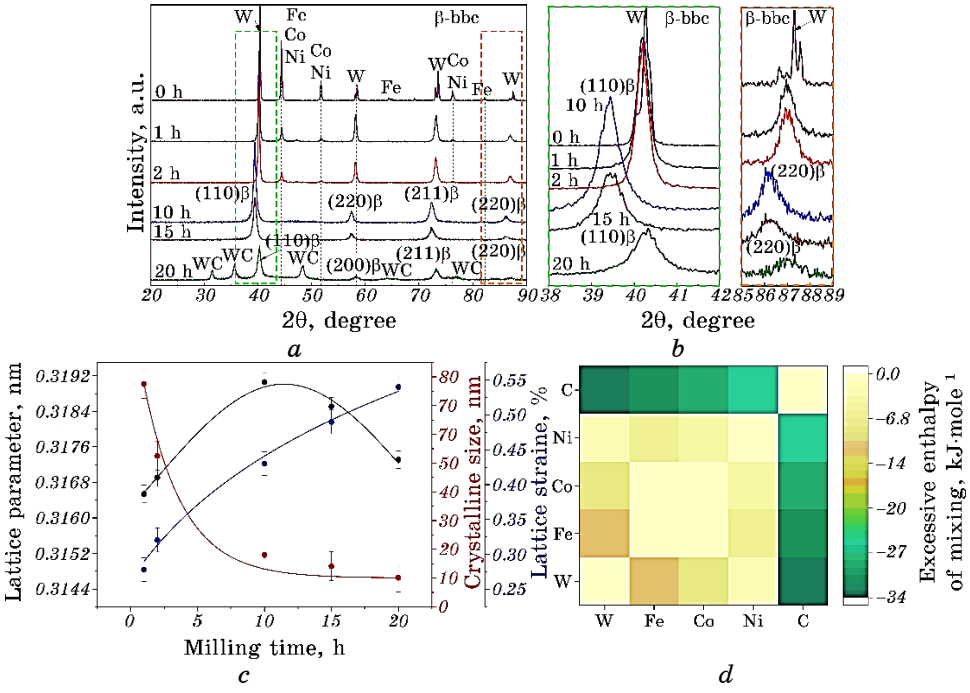


Fig. 1. XRD patterns of $W_{1.5}FeCoNi$ ball-milled powder *vs.* milling time (*a*), (*b*). (*c*) Lattice parameter, crystallite size and lattice strain of W-based b.c.c. solid solution of milled $W_{1.5}FeCoNi$ powders. (*d*) Excessive binary enthalpies of mixing estimated using Miedema's model [28–30].

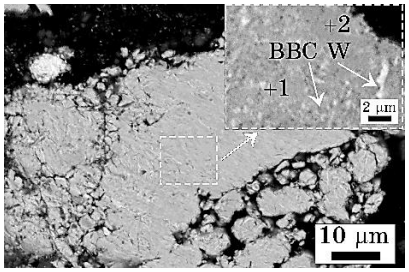
intensity of the diffraction peaks, can be observed (Fig. 1, *b*), which is associated with an increase in microstress level and refinement of the structure of powder particles (Fig. 1, *c*). The decrease in diffraction intensity and the disappearance of some diffraction peaks of Co, Ni, and Fe with the simultaneous slight shift of W peaks towards smaller 2θ angles due to the increase in lattice parameters (Fig. 1, *c*) can be considered as the beginning of alloying, dissolution of components, and the formation of solid solution. It should be noted that the dissolution of Fe, Co, and Ni atoms, which radii are smaller than that of W atom, should cause a decrease in the lattice parameter and a shift of peaks to larger angles. Yet, since the opposite is observed, it can be assumed that the dissolution of carbon atoms occurs and causes a slight increase in the lattice parameter of W.

Increasing the MA time to 10 h promotes the obtaining of b.c.c. solid solution. The positions of the β-phase peaks are close to those of W (Fig. 1, *a*, *b*), which suggests that the b.c.c. solid solution is formed, apparently, based on W crystal lattice. A significant shift of the β-phase peaks towards smaller 2θ angles and an increase in the lattice parameter due to the dissolution of carbon atoms are observed.

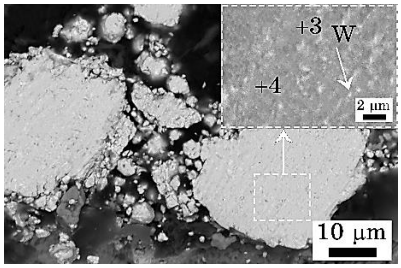
Further increase in MA time to 15 h does not change the phase composition of the alloy, but change the lattice parameter of b.c.c. solid solution. Compared to the previous MA stage, the lattice parameter decreased from 0.319 nm to 0.3184 nm (Fig. 1, *c*), which may be due to the beginning of the interaction of carbon atoms with tungsten. The significant decrement of diffraction intensity and peak broadening are observed (Fig. 1, *a*, *b*).

After 20 h of MA, significant changes are observed in the x-ray diffraction spectrum (Fig. 1, *a*). In addition to the reflections of the b.c.c. solid solution (β-phase), the diffraction lines corresponding to tungsten carbide are observed. This indicates that the MA process results in the *in situ* formation of WC phase which content in the alloy is 28.7 wt.%. The lattice parameter of b.c.c. solid solution decreases to 0.3169 nm, which is related to its depletion on W and C atoms owing to *in situ* formation of WC (Fig. 1, *c*). According to the binary enthalpy of mixing [28–30], W exhibits the most negative ΔH_{mix} values (Fig. 1, *d*) with carbon (–34 kJ·mol^{-1}), indicating the strongest chemical affinity and the highest tendency to form carbides. In contrast, the Fe–Co–Ni subsystem shows relatively small negative enthalpies of mixing, suggesting good mutual solubility and the formation of a homogeneous solid solution.

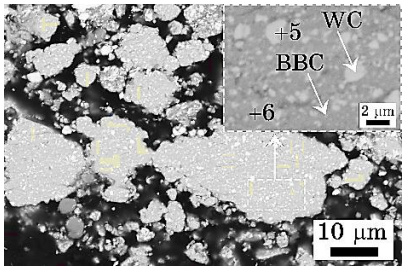
The SEM image of the ground and polisher powder surface is shown in Fig. 2. After 10 h of MA, the $W_{1.5}$FeCoNi alloy consists of a b.c.c. solid solution and the W particles (Fig. 2, *a*, *e*, points 1–2). Tungsten has one of the largest atomic radii in the W–Fe–Co–Ni system (139 pm) and the highest melting point; due to this, its dissolution can take



a



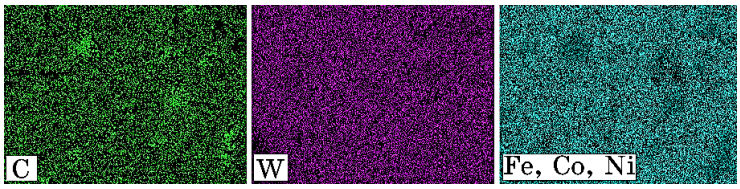
b



c

Points	Atomic, %					
	Fe	Co	Ni	W	C	O
1	1.1	3.2	2.5	77.7	5.4	10.1
2	20.0	20.5	20.1	35.5	1.5	2.4
3	18.5	22.4	22.1	36.1	0.2	0.7
4	3.4	6.0	5.4	73.6	3.2	8.4
5	0.5	0.8	0.2	48.4	50.0	0.1
6	16.7	22.2	21.8	38.0	0.5	0.8

e



d

Fig. 2. SEM image of cross-section of $W_{1.5}FeCoNi$ powder after mechanical allying at: (*a*) 10 h, (*b*) 15 h, (*c*) 20 h with (*d*) elemental mapping analysis for the *in situ* reacted $W_{1.5}FeCoNi$ + C and local point analysis for different alloying time (*e*).

the longest time. Increasing MA time to 15 h promotes homogenization of the microstructure and a decrease of quantity the amount and size of W particles. At final stage of MA (20 h), the powder microstructure consists of b.c.c. solid solution and WC particles (Fig. 2, *c*–*e*) with an average size of 0.75 μm.

During MA process, carbon atoms contained in the petrol were dissolved in the metal powder mixture, which resulting in a high carbon concentration in $W_{1.5}FeCoNi$ alloy. The carbides were formed by W interacting with the carbon in the petrol after long-time high-energy ball milling. A similar observation of carbide formation was reported, when fabricating the AlFeMgTiZn [31] and MoNbTaW [25] alloys by ball milling, and the carbides were formed due to the presence of stearic acid as processing controlling agent.

Based on the XRD patterns (Fig. 1) and SEM images (Fig. 2) of MA powder, the mechanism of WC formation was suggested (Fig. 3). The initial portion of powder on Stage 1 (near 1–2 hours of MA) undergoes dynamic solid-state interaction processes under high local deformation and heating. At this stage, in addition to grinding and reducing the average size of crystallites (Fig. 1, *c*), the processes of cold welding and overlapping of powder particles occur [32]. During MA, the organic components of petrol undergo gradual decomposition due to the intense mechanical energy input. In the initial 1–5 hours of milling, gasoline largely retains its molecular structure, with minimal bond breakage. At Stage 2 (MA, 10 h), the powder alloy, in addition to b.c.c. phase, contains non-reacted W particles. The organic component can homolytically cleave C–C and C–H bonds, generating free radicals and small-unsaturated hydrocarbons such as alkenes [33]. The transformation in petrol associated with the intensive mechanical impact during MA, especially by the high-energy collisions between milling media and powder particles, creates localized extreme conditions (high pressure, shear stress, and transient temperature spikes), which are sufficient to break chemical bonds [34]. Under these conditions, some part of carbon can be dissolved in the b.c.c. lattice. At Stage 3 (MA, 15 h), the final phase of breaking the C–C bonds and the formation of graphite nanolayers in the form of coke may occur.

Since during mechanical alloying W particles can remain in a dispersed state in the matrix of the b.c.c. solid solution, the *in situ* formation of WC at Stage 4 can have two paths. First way, it is a reaction of carbon with a W-based b.c.c. solid solution. The C diffuses into the b.c.c. lattice and reacts with W, forming dispersed WC particles (less

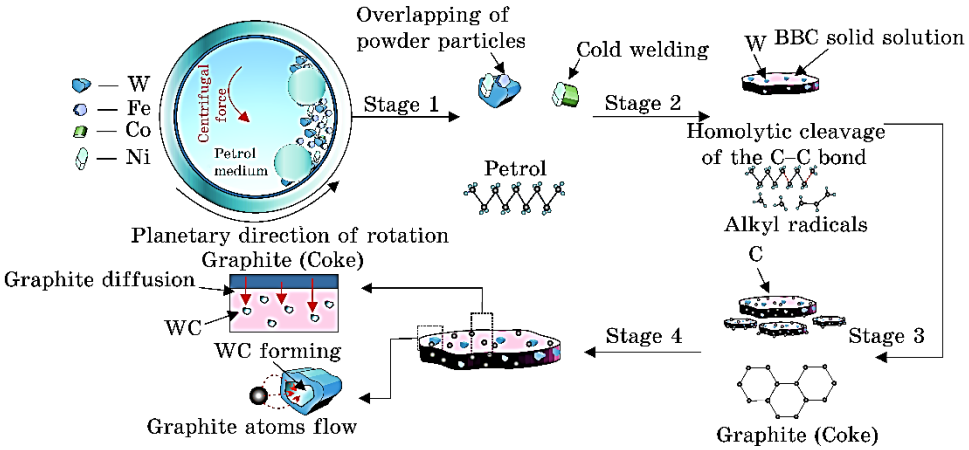


Fig. 3. The mechanism of WC *in situ* formation during mechanical alloying of $W_{1.5}$FeCoNi in the petrol medium.

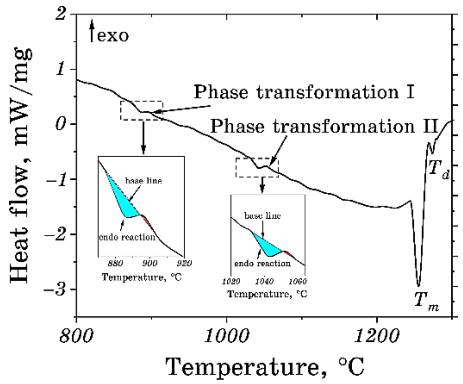


Fig. 4. DSC curves of 20 h mechanically alloyed $W_{1.5}$FeCoNi alloy.

than 0.5 μm in size). Second, it is the direct reaction between carbon and the residual W. In this way, the particle size of WC is of around 1 μm.

In order to investigate the phase transformations and melting point of $W_{1.5}$FeCoNi alloy, DSC analysis was carried out, and the results are presented in Fig. 4. During heating, two pairs of endothermic (885°C and 1040°C) peaks were indicated. At 885°C, the endothermic reaction is associated with a short-range ordering effect [35], sintering of alloy powder during heating, and secondary WC precipitation by carbon dissolution from the b.c.c. lattice. The next endothermic effect started at 1028°C indicates the randomization of the solid solution, segregation and particular b.c.c.–f.c.c. transformation. The b.c.c. lattice has more open structure; the elements, especially with small atomic radii diffused more easily as compared to f.c.c. structure [36]. The melting point of the $W_{1.5}$FeCoNi alloy is of 1250°C. Increasing the temperature promotes the thermal degradation of MEH (T_d point, Fig. 4), because the melt reacts with the crucible and the moisture in argon.

4. CONCLUSIONS

In summary, an *in situ* WC-reinforced $W_{1.5}$FeCoNi medium-entropy alloy was successfully fabricated by mechanical alloying in a high-carbon (petrol) medium. The process led to the formation of a b.c.c. solid solution matrix and dispersed WC particles, with particle sizes ranging from 0.5 to 1 μm. The WC formation occurs *via* two mechanisms: diffusion of carbon into the b.c.c. lattice and reaction with residual W atoms. XRD and SEM analyses confirmed progressive alloying, crystallite refinement and homogenization of the structure over 20 h of milling. DSC analysis revealed two endothermic peaks at 885°C and 1040°C, attributed to short-range atomic ordering, powder sinter-

ing, secondary WC precipitation, and randomization of the solid solution including partial b.c.c.–f.c.c. transformations. The study demonstrates that high-energy mechanical alloying in a carbon-rich environment is an effective strategy to produce MEAs multicomponent alloys with *in situ* carbide reinforcement, offering potential for improved mechanical properties and high-temperature performance.

ACKNOWLEDGMENTS

This work was supported by the National Research Foundation of Ukraine (project No. 2023.03/0053, Agreement No. 197.03/0053).

AUTHOR CONTRIBUTIONS

Teslia S. Yu.: conceptualization of the study, development of the methodology, conducting the research, analysis and interpretation of the results, preparation of the initial manuscript draft, and data visualization; Yurkova O. I.: conducting the research, data processing and systematization, validation of the results, preparation of the initial manuscript draft, editing and revision of the text; Leonov D. S.: preparation of the manuscript, editing of the manuscript; Loboda P. I.: conducting the research, organization of the study, and scientific supervision of the research. All authors approved the final version of the manuscript.

REFERENCES

1. Jien-Wei Yeh, S.-K. Chen, Su-Jien Lin, Jon-Yiew Gan, Tsung-Shune Chin, Tian Shun, C.-H. Tsau, and S. Y. Chang, *Adv Eng Mater*, **6**, No. 5: 299 (2004).
2. Modupeola Dada, Patricia Popoola, and Ntombi Mathe, *World Journal of Engineering*, **20**, Iss. 1: 43 (2023).
3. Daniel B. Miracle, Ming-Hung Tsai, Oleg N. Senkov, Vishal Soni, and Rajarshi Banerjee, *Scr Mater*, **187**: 445 (2020).
4. Yiping Lu, Yong Dong, Sheng Guo, Li Jiang, Huijun Kang, Tongmin Wang, Bin Wen, Zhijun Wang, Jinchuan Jie, Zhiqiang Cao, Haihui Ruan, and Tingju Li, *Scientific Reports*, 4, Article No. 6200 (2014).
5. George J. Wise, Nicole L. Church, Hon Tong Pang, Robert P. Thompson, Howard J. Stone, and Nicholas G. Jones, *Adv. Eng. Mater*, **27**, Iss. 9: 2402330 (2025).
6. Ping'an Zang, Zhaoqiang Chen, Mingdong Yi, Hui Chen, Kun Dong, Jingjie Zhang, Guangchun Xiao, Xianglong Meng, and Chonghai Xu, *Ceramics International*, **51**, Iss. 12, Part A: 16234 (2025).
7. Zijian Wang, Fei Xing, Guojian Xu, Weijun Liu, and Hongyou Bian, *Mater Today Commun*, **49**: 113991 (2025).
8. Yunfei Cheng, Chaohui Wang, Meiling Dong, Yuan You, Weidong Cheng,

Wanjun Xie, Zhenwei Wang, Liang Wang, Xiaodong Zhang, and You Wang, *Intermetallics (Barking)*, **187**: 109003 (2025).
9. Muhammed Muneer S, Arun B. S, Renjish Vijay, Aju Kumar V. N, Anand Sekhar R, *Results in Surfaces and Interfaces*, **20**: 100622 (2025).
10. J. G. Lopes, A. Candeias, P. Agrawal, J. Shen, N. Schell, R. S. Mishra, and J. P. Oliveira, *J. Alloys Compd.*, **995**: 174694 (2024).
11. Yu Yin, Yitian Zhao, Kai En Koey, Qiyang Tan, Ming-Xing Zhang, and Han Huang, *Composites Part B: Engineering*, **235**: 109795 (2022).
12. Hui Liang, Jingzhuo Zhang, Jinxin Hou, Jingchang Sun, Jianhong Liu, Jiawen Liu, Xu Han, Jiani Tan, Li Jiang, Xiaocong Li, and Zhiqiang Cao, *Journal of Materials Research and Technology*, **38**: 1014 (2025).
13. Lijun Wang, Lulu Guo, Huicong Chen, Chenwei Shao, Zhaoying Ding, Hyun Suk Choi, Maxx Yao, and Yu Zou, *Intermetallics (Barking)*, **186**: 108964 (2025).
14. Xinggang Wang, Meng Sun, Jiaxin Liu, Xueqing Liu, Weibin Jiang, Xianping Wang, and Qianfeng Fang, *Crystals*, **14**, Iss. 12: 1029 (2024).
15. L. Chmielak, L. Mujica Roncery, P. Niederhofer, S. Weber, and W. Theisen, *SN Applied Sciences*, **3**: Article No. 835 (2021).
16. Tuanwei Zhang, Renlong Xiong, Jae Wung Bae, Peyman Asghari-Rad, Soung Yeoul Ahn, Huabei Peng, Zhihua Wang, and Hyoung Seop Kim, *Journal of Alloys and Compounds*, **1003**: 175698 (2024).
17. Yang Lan, Yong Zhang, Yingbo Peng, Andong Wang, Yuan Gao, Wenfei Yang, Weijie Fan, Wei Zhang, and Yong Liu, *Journal of Alloys and Compounds*, **990**: 174400 (2024).
18. Mateusz Włoczewski, Kinga Jasiewicz, Piotr Jenczyk, Elżbieta Gadalińska, Krzysztof Kulikowski, Yong Zhang, Rui Xuan Li, and Dariusz M. Jarząbek, *Metallurgical and Materials Transactions A*, **56**: 2040 (2025).
19. Tinghui Cao, Yake Wu, Jin Tian, Feng Jiang, and Jun Sun, *Scr. Mater.*, **215**: 114692 (2022).
20. Jie Lu, Ying Chen, Ling Li, Han Zhang, Xiancheng Zhang, and Xiaofeng Zhao, *Composites Part B: Engineering*, **265**: 110933 (2023).
21. Bharat Gwalani, Rizaldy M. Pohan, Junho Lee, Bin Lee, Rajarshi Banerjee, Ho Jin Ryu, and Soon Hyung Hong, *Scientific Reports*, **8**: Article No. 14085 (2018).
22. M. Adil Mehmood, Khurram Shehzad, M. Mujahid, Talha Bin Yaqub, Andy Godfrey, Filipe Fernandes, F. Z. Muhammad, and Khurram Yaqoob, *Scientific Reports*, **12**: Article No. 21486 (2022).
23. M. Y. He, Y. F. Shen, N. Jia, and P. K. Liaw, *Appl Mater Today*, **25**: 101162 (2021).
24. Yemao Lu, Andrey Mazilkin, Torben Boll, Nikita Stepanov, Sergei Zherebtzov, Gennady Salishchev, Éva Ódor, Tamas Ungar, Enrique Lavernia, Horst Hahn, and Yulia Ivanisenko, *Materialia*, **16**: 101059 (2021).
25. Congyan Zhang, Uttam Bhandari, Jialin Lei, Congyuan Zeng, Shengmin Guo, Hyunjoo Choi, Seungjin Nam, Jinyuan Yan, Shizhong Yang, and Feng Gao, *Crystals*, **11**, Iss. 9: 1073 (2021).
26. Zhufeng He, Nan Jia, Haile Yan, Yongfeng Shen, Mingwei Zhu, Xianjun Guan, Xiaoli Zhao, Shenbao Jin, Gang Sha, Yuntian Zhu, and Chain T. Liu, *International Journal of Plasticity*, **139**: 102965 (2021).
27. Meiyan Feng, Tianxiang Lin, Guofu Lian, Changrong Chen, and Xu Huang,

Ceram. Int., **50**, Iss. 24, Part C: 55286 (2024).
28. Lihui Tian, Ming Fu, and Wei Xiong, *Materials*, **11**, Iss. 2: 320 (2018).
29. Long Wu, Aimin Wang, and Wenhao Xing, *Metals (Basel)*, **13**, Iss. 5: 987 (2023).
30. Te-Kang Tsao and An-Chou Yeh, *Materials Transactions*, **56**, Iss. 11: 1905 (2015).
31. Vincent H. Hammond, Mark A. Atwater, Kristopher A. Darling, Hoang Q. Nguyen and Laszlo J. Kecskes, *JOM*, **66**: 2021 (2014).
32. L. Lü and M. O. Lai, *Mechanical Alloying* (New York: Springer: 1998).
33. Nida Tasneem, Shakeel Ahmed, and Mohammad M. Hossain, *Arabian Journal for Science and Engineering*, **50**: 3649 (2024).
34. Challapalli Suryanarayana, *Research*, **2019**: Article ID 4219812 (2019).
35. Angelo F. Andreoli, Andrea Fantin, Sergey Kasatikov, Vinícius P. Bacurau, Michael Widom, Piter Gargarella, Eric M. Mazzer, Thomas G. Woodcock, Kornelius Nielsch, and Francisco G. Coury, *Materials & Design*, **238**, Article No. 112724 (2024).
36. Marek Zajusz, Monika Jawańska, Juliusz Dąbrowa, Katarzyna Berent, Grzegorz Cieślak, Tadeusz Kulik, and Krzysztof Mroczka, *Mater. Res. Lett.*, **10**: No. 8: 556 (2022).